

# The Nucifer Reactor Neutrino Monitor

J. Bazoma<sup>d</sup>, G. Boireau<sup>a</sup>, L. Bouvet<sup>a</sup>, C. Buck<sup>e</sup>, V.M. Bui<sup>d</sup>, A. Collin<sup>a</sup>, V. Communeau<sup>d</sup>, S. Cormon<sup>d</sup>, G. Coulloux<sup>a</sup>, M. Cribier<sup>a,f</sup>, A. Cucoanes<sup>a,d</sup>, H. Deschamp<sup>a</sup>, E. Dumonteil<sup>c</sup>, V. Durand<sup>a,f</sup>, M. Fallot<sup>d</sup>, M. Fechner<sup>a</sup>, V. Fischer<sup>a</sup>, J. Gaffiot<sup>a</sup>, M. Gautier<sup>d</sup>, L. Giot<sup>d</sup>, B. Guillon<sup>d</sup>, G. Guilloux<sup>d</sup>, R. Granelli<sup>a</sup>, J. Haser<sup>e</sup>, Y. Kato<sup>a</sup>, T. Lasserre<sup>a,f</sup>, L. Latron<sup>a</sup>, P. Legou<sup>a</sup>, M. Lenoir<sup>d</sup>, A. Letourneau<sup>a</sup>, D. Lhuillier<sup>a</sup>, M. Lindner<sup>e</sup>, J. Martino<sup>d</sup>, G. Mention<sup>a</sup>, G. Mercier<sup>d</sup>, T. Mueller<sup>a</sup>, T-A. Nghiem<sup>a</sup>, A. Onillon<sup>d</sup>, N. Pedrol<sup>a</sup>, J. Pelzer<sup>a</sup>, M. Pequignot<sup>a</sup>, Y. Piret<sup>a</sup>, N. Pleurel<sup>d</sup>, A. Porta<sup>d</sup>, G. Prono<sup>a</sup>, L. Scola<sup>a</sup>, P. Starzinski<sup>a</sup>, C. Varignon<sup>b</sup>, Th. Vilajosana<sup>d</sup>, M. Vivier<sup>a</sup>, and F. Yermia<sup>d</sup>  
(Nucifer collaboration)

<sup>a</sup> Commissariat à l'Énergie Atomique et aux Énergies Alternatives,  
Centre de Saclay, DSM/IRFU, 91191 Gif-sur-Yvette, France

<sup>b</sup> Commissariat à l'Énergie Atomique et aux Énergies Alternatives,  
Centre de Saclay, DAM, 91191 Gif-sur-Yvette, France

<sup>c</sup> Commissariat à l'Énergie Atomique et aux Énergies Alternatives,  
Centre de Saclay, DEN, 91191 Gif-sur-Yvette, France

<sup>d</sup> Subatech, CNRS/IN2P3, F-44307 Nantes, France

<sup>e</sup> Max-Planck-Institut für Kernphysik, 69029 Heidelberg, Germany

<sup>f</sup> Laboratoire AstroParticule et Cosmologie, 75231 Paris cedex 13, France

**Abstract.** The detection of electron antineutrinos emitted in the decay chains of the fission products in nuclear reactors associated with accurate simulations provides an efficient method to assess both the thermal power and the evolution of the core fuel composition. These information are considered to be used for safeguarding civil nuclear reactors in the future. The Nucifer experiment aims to demonstrate the concept of neutrino metrology at the pre-industrialized stage. A novel detector has been designed to meet IAEA requirements detector and it has been deployed at 7 m away from the Osiris research reactor at CEA-Saclay in France. We report the detector performances and the first detection of neutrinos.

## 1. Introduction

Neutrino detectors have unique abilities to non-intrusively monitor a nuclear reactor's operational status, power and fissile content in real-time, from outside the reactor containment without being tampered. From the confirmation of the absence of unrecorded production of fissile material in declared reactors to the estimation of the total burn-up of a reactor core, they could have a considerable value in bulk process and safeguards by design approaches for new and next generation reactors. The detection of electron antineutrinos emitted in the decay chains of the fission products in nuclear reactors associated with accurate simulations provides an efficient method to assess both the thermal power and the evolution of the fuel composition. Nucifer is a detector specifically built for robust, long-term safeguards measurements of these metrics close to operating reactors. The Nucifer experiment aims to demonstrate the concept of neutrino metrology at the pre-industrialized stage. We report here the first detection of neutrinos with the Nucifer detector located at 7 m away from the Osiris research reactor at CEA-Saclay.

## 2. Reactor and expected neutrino flux

### 2.1. The Osiris reactor

Osiris is an experimental reactor located within the Saclay center of CEA and designed for technological irradiation purposes and radioisotopes production [1]. It is a light water reactor of open-core pool type, operated at a thermal power of 70 MW, and producing high neutron flux in the core (of a few  $10^{18}$  neutrons/m<sup>2</sup>/s both in the thermal and fast energy range). The compact design of the core ( $80 \times 70 \times 70$  cm, including the vessel) helps reducing uncertainties due to the neutrino propagation length also called baseline.

### 2.2. Expected neutrino flux

The emitted antineutrino flux arises from the fissions of mainly <sup>235</sup>U isotopes. The number of neutrino events per day depends on the baseline of the experiment, the number of target protons, the detector efficiency and the flux emitted from the Osiris reactor. The flux depends on its thermal power and the energy released per fission and cross section per fission of the fissioning isotope.

The rates and associated errors of <sup>235</sup>U fissions were deduced to compute the associated antineutrino flux. To this aim, we have used the recently improved spectra from [2], converted from the ILL reference spectra [3].

The thermal power of the Osiris reactor is measured at the 2% level at 70 MW [4].

## 3. Detector description

### 3.1. The Nucifer detector

The Nucifer detector system (FIG. 1) consists of a neutrino target detector, an active veto to tag the muon induced backgrounds, 14 cm of Polyethylene to shield the target against neutrons and a 10 cm lead layer to stop gamma rays. An extra 10 cm lead wall has been erected on the reactor side to further shield reactor-induced gamma rays.

The neutrino target is contained inside a cylindrical double-vessel made of stainless steel (height 1.8 m, diameter 1.2 m) with a diffusive internal surface to increase light collection. The tank is filled with 0.85 m<sup>3</sup> of Gadolinium-doped (Gd) liquid scintillator.

The chemistry of the Nucifer scintillator is based on a development for the target liquid of the Double Chooz reactor neutrino experiment. The Gd is dissolved in the organic liquid in the form of a Gd-beta-diketonate complex. The focus in the scintillator design was on long-term stability over several years and chemical purity. In order to better reject backgrounds, the Gd-concentration was increased to about 0.2% and the o-PXE (ortho-Phenylxylylethane) concentration was raised to about 50% with respect to the n-dodecane concentration.

Sixteen 8-inch (20 cm) photomultiplier tubes (PMTs) located at the top of the detector vessel ensure an efficient light collection. A 25 cm thick acrylic disk optically couples the PMTs with the liquid surface while shielding the intrinsic PMT radioactivity from the scintillator and ensuring a more uniform response in the whole target volume. A LED based light injection system allows monitoring the PMT gains and possible instrumental drifts. In

addition small encapsulated radioactive sources can be deployed along the target central axis inside a vertical tube.

The veto design is based on a novel concept: 32 modular detectors, each one containing a 5 cm thick plastic scintillator of 150 to 170 cm length and 25 cm large observed by one PMT decoupled from its surface. The scintillator thickness was chosen in order to discriminate cosmic muons from gamma rays and the selected threshold allows a muon detection efficiency greater than 95%.

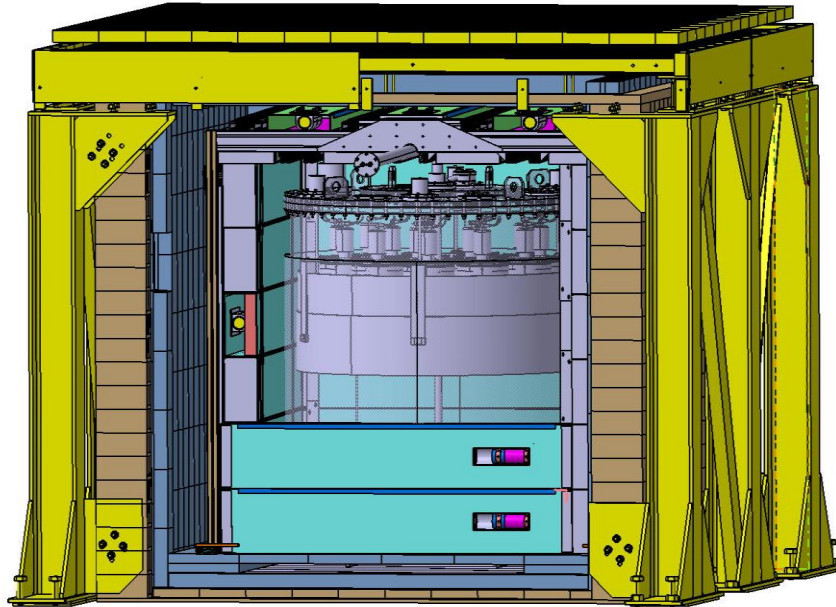


*FIG. 1. Drawing of the Nucifer detector. The overall footprint is about  $3 \times 3 \text{ m}^2$ .*

### **3.2. Data acquisition and monitoring**

The Data Acquisition system (DAQ) is based on the Lab-View [5] software allowing a remote control of the acquisition and a constant monitoring of the safety parameters, such as pressure, liquid level and temperature via several sensors. In case of a significant deviation of one detector parameter, warning emails are automatically sent to on-call experts before the deviation reaches the threshold of an alarm in the reactor control room.

The Nucifer detector has been operated with no security failure since its installation at Osiris in spring 2012.

## **4. Calibration**

The calibration system was designed to give an absolute energy scale to the light response of the detector and to check the linearity and the stability of the whole system all along the experiment. It is made of Light-Emitting Diodes (LED) deployed within the Nucifer tank via optical fibers and radioactive sources.

### **4.1. Light injection with diodes**

The Nucifer tank is equipped with 7 Teflon light diffusers, linked by optical fibers to Light-Emitting Diodes (LED) located in the electronic rack and controlled through the acquisition

software. One of this LED is used to generate Single Photo-Electrons (SPEs) on the PMTs, 4 are used with different intensities to test the linearity and stability of the PMTs on their whole response range, and the last 2 are spares.

This system allows the measurement of pedestal and gain for each channel and each run, thanks to an automatic fit of the pedestal and of the SPE signals. Each run and channel is therefore auto-calibrated in photo-electrons (p.e.), allowing a proper sum of the 16 PMT charges.

The detector response to multiple LED patterns compared to the equivalent sum of single LED patterns demonstrates linearity at the 1% level in the 2-8 MeV<sup>1</sup> detection range. The uncertainty on pedestal is below 1% for each run although large drifts due to temperature changes in the electronic rack are observed on a daily basis. The run-to-run gain fluctuations rise to 2.5%, due to the difficult fit of the SPE signal. This signal is indeed limited on few acquisition channels because of the overall large dynamic to be treated. Apart from these statistical fluctuations, the gains have shown remarkable stability over more than 2 years of running. No drift in detector response to LED patterns has been shown either.

#### ***4.2. Energy scale***

Small encapsulated radioactive sources can be deployed inside a vertical tube along the target central axis. Three gamma-emitting sources (<sup>137</sup>Cs, <sup>60</sup>Co and <sup>22</sup>Na) and one neutron source (<sup>241</sup>Am-Be), each of few kBq, are used. While the first three deliver gammas from 661 to 1332 keV, the Americium-Beryllium (Am-Be) source emits a neutron in coincidence with a gamma ray of 4.4 MeV for around 3/4 of the events. This source is used to study the detection of two correlated energy depositions, similar to the expected neutrino signal. It also allows checking the rejection efficiency of the fast neutrons background by pulse shape analysis.

These sources were placed at different vertical locations in the detector and used to calibrate the energy scale of the light response. A global calibration factor of about 340 p.e./MeV was obtained. The energy resolution is dominated by edge effects of the small target volume (energy loss due to escaping gamma rays and light absorption on the vessel walls).

### **5. Analysis**

The signature of antineutrino events in Nucifer consists of a delayed coincidence between a prompt energy deposition by the positron, and a later energy deposition due to the neutron capture on Gd within a short time window. This is the Inverse Beta Decay (IBD) reaction. The basis of the analysis is to compare the number of antineutrinos detected to the predictions based on the reactor data. We thus need to separate the IBD events from the background due to random coincidences and correlated coincidences induced by cosmic muons and potentially the reactor core.

#### ***5.1. Data Sample***

A typical Osiris running cycle consists of three weeks with the reactor at full power (ON) followed by a week of shutdown period (OFF). A quality check is performed on a run-by-run basis, rejecting data not complying with requirements on gain and LED response stability. Transient periods at start and end of the cycles are analyzed separately.

---

<sup>1</sup> 1 MeV = 10<sup>6</sup> eV = 1.6 10<sup>-13</sup> Joules

## 5.2. Accidental background

Accidental background is caused when two random energy depositions occur within the time window of interest for signal selection. In Nucifer, they usually originate from a gamma ray followed by an independent neutron capture on Gd or from two independent gamma rays. To investigate this background, it is worth looking at the energy spectrum of single energy depositions.

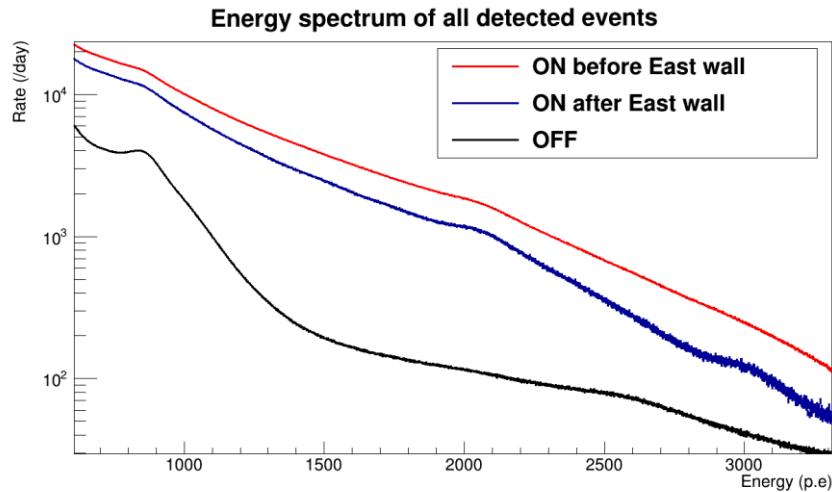


FIG. 2. Energy spectrum of the singles event rate at reactor full power (70 MW) before and after the new east lead wall installation and during reactor OFF combined periods

When the reactor is stopped, the event rate is dominated by low energy natural radioactivity decays. However, when the reactor is in operation, unexpected features are showing up. A bump at 6 MeV and a falling spectrum up to 12 MeV are observed. Whereas the reactor is located in the east direction, this excess of events comes mainly from the south. Investigations revealed the existence of a primary water loop of the main reactor cooling circuit, located behind the 1 m thick concrete south wall of the detector casemate. The water of this circuit is highly activated by the fast neutron flux inside the core. It produces  $^{16}\text{N}$  from  $^{16}\text{O}$  activation, which subsequently decays with a 7.13 s half-life emitting a 6.1 MeV gamma ray.

To reduce this background a new 10 cm thick lead wall was built on the south side of the detector dramatically reducing the  $^{16}\text{N}$  background by a factor  $\sim 100$ . From this moment on, the event rate is a smooth exponential decay from the threshold until energies higher than 10 MeV, where the cosmic tail is reached.

The background is now dominated by reactor-induced gammas, with a prejudicial significant rate at high energy, attributed to radiative neutron capture on metallic structures close to the detector. After the first cycle, a 4 cm additional thick lead screen was installed between the reactor and the detector, further reducing the accidental background, by a factor of 3, as displayed in FIG. 2.

Despite this high event rate the accidental background can be precisely measured in-situ and subtracted from the overall signal. This way the final uncertainty induced by the accidentals is the purely statistical fluctuation of the accidental rate on top of the signal of correlated pair of events.

### 5.3. Cosmogenic induced background

In the case of correlated background, a single physical process is the origin of two consecutive energy depositions in the detector. The correlated background is mainly induced by fast neutrons created in inelastic muon interactions (spallation). They scatter off protons in the detector's target providing prompt-like energy depositions and end up being captured on Gd nuclei, providing delayed-like events.

The majority of atmospheric muons travels through the shallow overburden of the Osiris site (about 10 meter water equivalent). However the high efficiency of the muon veto system allows their tagging with a 97% efficiency. The majority of the spallation fast neutrons are removed from the data sample by discarding the events occurring within 0.1 ms after each recorded muon. When a nearby muon interaction is not tagged by the muon veto about 2/3 of the fast neutrons reaching the Nucifer target are rejected using Pulse Shape Discrimination (PSD). This PSD is based on the fact that in our liquid scintillator, the signal associated to a fast neutron has a slower tail than in the case of a positron signal (associated to a neutrino interaction). Then the observed good stability of the detector allows an efficient subtraction of the remaining constant cosmogenic correlated background from the reactor ON data.

### 5.4. Neutrino signal

The selection of neutrino candidates is based on 3 different selection criteria based on energy, time and PSD cuts. The prompt event energy is requested to lie between 2 and 7.1 MeV; the delayed event energy has to be included between 4.2 and 9.6 MeV. The delayed event time must lie alone within 40  $\mu$ s time windows before and after the prompt event. This range corresponds to 3 times the neutron capture time on Gd and hence reject possible multiple neutrons induced by a muon. Finally, the muon veto signal, handled at the level of the offline analysis, prevents any event to be considered sooner than 100  $\mu$ s after a muon is tagged.

The detection efficiency is defined as the ratio of the number of simulated events passing all the analysis selection cuts to the total number of neutrino vertices generated. Using TRIPOLI4 [6] and GEANT4 [7] simulations, the global detection efficiency is found to be  $32.0 \pm 2.0$  %.

### 5.5. Results

The time evolution of the detected neutrino rate is shown on FIG. 3. The orange curve is the predicted neutrino. The dotted points represent the measured daily rates after subtraction of the accidental background.

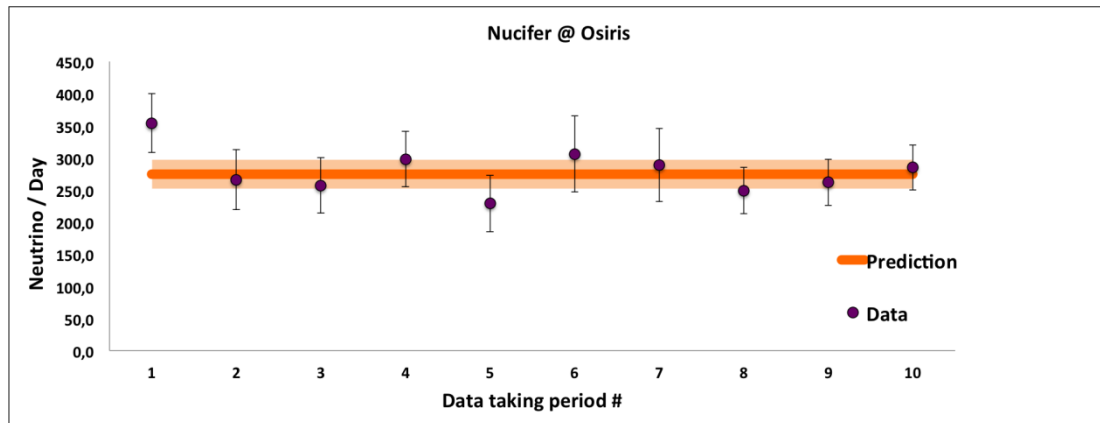


FIG. 3. Antineutrino rate measurement of the Osiris nuclear reactor operations.

Finally the mean observed rate of  $276 \pm 14$  neutrinos/day is found in good agreement with the predicted rate of  $274 \pm 23$  neutrinos/day. A confidence level of 95% on the detection of neutrinos coming from the reactor can be reached in less than 12 hours. It already provides a decent monitoring of the reactor activity despite the current high level of accidentals during reactor ON periods due to the extreme proximity to the reactor core.

## **6. Conclusion**

The Nucifer detector has been running smoothly since spring 2012 without showing any instabilities or loss of performances. Its remote controllability and efficient data acquisition chain allow a direct measurement of the neutrino flux and therefore a real-time determination of the reactor fuel content. Its shallow depth and proximity to the reactor imply an important work on the analysis and background subtraction. While showing the difficulty of installing a neutrino detector in the vicinity of a reactor, the Nucifer detector managed to detect a significant rate of antineutrinos thus leading the way for future detectors dedicated to nuclear safeguards within the IAEA standards. We conclude that the Nucifer detector could safely and efficiently in the vicinity of a nuclear power station, free of the current dominant reactor-induced background.

## REFERENCES

- [1] Direction de l'Énergie Nucléaire (DEN), Direction Déléguée aux Affaires Nucléaires de Saclay (DANS), Département des Réacteurs et Services Nucléaires (DRSN) : Le réacteur Osiris. Les éditions stratégiques.  
[http://nucleaire.cea.fr/fr/publications/pdf/osiris\\_plaquette\\_FR.pdf](http://nucleaire.cea.fr/fr/publications/pdf/osiris_plaquette_FR.pdf).
- [2] P. Huber: On the determination of anti-neutrino spectra from nuclear reactors. *Phys. Rev.*, C84:024617, 2011.
- [3] K. Schreckenbach et al.: Determination of the antineutrino spectrum from U-235 thermal neutron fission products up to 9.5 MeV. *Phys. Lett.*, B160:325–330, 1985.
- [4] J. Pelzer, Internship report, 2012.
- [5] Chance Elliott, Vipin Vijayakumar, Wesley Zink, and Richard Hansen: National Instruments LabVIEW: A Programming Environment for Laboratory Automation and Measurement *Journal of Laboratory Automation* February 2007 12: 17-24,  
doi:10.1016/j.jala.2006.07.012
- [6] Emeric BRUN, Frederic DAMIAN, Eric DUMONTEIL, Francois-Xavier HUGOT, Yi-Kang LEE, Fausto MALVAGI, Alain MAZZOLO, Odile PETIT, Jean-Christophe TRAMA, Thierry VISONNEAU, Andrea ZOIA: TRIPOLI-4 version 8 User Guide, CEA-R-6316, Feb. 2013.
- [7] A. Afanaciev et al.: Geant4: A toolkit for the simulation of the passage of particles through matter. <http://geant4.cern.ch/>.